

Reparametrization of the Karplus Relation for $^3J(\text{H}^\alpha\text{--N})$ and $^3J(\text{H}^{\text{N}}\text{--C}')$ in Peptides from Uniformly $^{13}\text{C}/^{15}\text{N}$ -Enriched Human Ubiquitin

Andy C. Wang and Ad Bax*

Contribution from the Laboratory of Chemical Physics, National Institute of Diabetes and Digestive and Kidney Diseases, National Institutes of Health, Bethesda, Maryland 20892-0520

Received October 5, 1994[⊗]

Abstract: The Karplus relations for vicinal J couplings, which relate the peptide backbone angles ϕ and ψ to $^3J(\text{H}^\alpha\text{--N})$ and $^3J(\text{H}^{\text{N}}\text{--C}')$, have been reparametrized on the basis of measurements made on uniformly $^{13}\text{C}/^{15}\text{N}$ -enriched human ubiquitin and backbone angles derived from the 1.8 Å X-ray structure of this protein (Vijay-Kumar, S.; Bugg, C. E.; Cook, W. J. *J. Mol. Biol.* **1987**, *194*, 531–544). For $^3J(\text{H}^\alpha\text{--N})$, values measured using an E.COSY-type HCACO experiment fall in the -1.9 to 0.1 Hz range and are described by the following: $^3J(\text{H}^\alpha\text{--N}) = -0.88 \cos^2(\psi + 60^\circ) - 0.61 \cos(\psi + 60^\circ) - 0.27$. The root-mean-square difference (rmsd) between measured values and the Karplus relation is 0.16 Hz. Values measured for $^3J(\text{H}^{\text{N}}\text{--C}')$ using an E.COSY-type HNCA experiment fall in the -0.4 to 3.6 Hz range, are described by $4.0 \cos^2(\phi) + 1.1 \cos(\phi) + 0.1$, and fit the observed J couplings with an rmsd of 0.45 Hz.

The importance of three-bond J couplings for determining three-dimensional molecular conformation by NMR methods is well-established. For peptides and proteins a wide variety of different J couplings is readily accessible and is commonly being used in the structure determination process. For most common types of three-bond J couplings the Karplus equation,¹ which correlates J with the intervening torsion angle, has been parametrized on the basis of conformationally constrained small molecules with similar patterns of substituents as the molecule of interest.² A more direct approach was used by Pardi et al.,³ who parametrized the Karplus relation for $^3J(\text{H}^{\text{N}}\text{--H}^\alpha)$ by relating the J values measured for peptide amides in pancreatic trypsin inhibitor to the dihedral angles available from high-resolution crystallographic studies. Very similar values for the Karplus coefficients describing $^3J(\text{H}^{\text{N}}\text{--H}^\alpha)$ were also derived using a range of other proteins.^{4,5} The present paper describes use of the same approach to parametrize Karplus equations for $^3J(\text{H}^{\text{N}}\text{--C}')$ and $^3J(\text{H}^\alpha\text{--N})$, which are related to the peptide backbone angles ϕ and ψ , respectively. Our study uses a sample of human ubiquitin, a protein which commercially can be obtained uniformly enriched with ^{13}C and ^{15}N (VLI Research, Southeastern, PA) and for which a high-resolution crystal structure is available.⁶

In peptides and proteins the most common ways to measure heteronuclear J couplings are E.COSY-based techniques⁷ and quantitative J correlation,⁸ a method in which the strength of a long-range correlation is related in a simple manner to the intensity of the corresponding cross peak. For measurement

of J couplings that are more than an order of magnitude smaller than the transverse relaxation rate of the observed nucleus, the E.COSY technique generally yields better results. E.COSY-based techniques require three magnetically active nuclei, say $^1\text{H}^\alpha$, $^{13}\text{C}'$, and ^{15}N . If the spin state of the ^{15}N is left unperturbed during an experiment in which $^1\text{H}^\alpha$ is correlated with $^{13}\text{C}'$ (in, for example, an HCACO experiment⁹), two cross peaks are obtained for each $^1\text{H}^\alpha\text{--}^{13}\text{C}'$ correlation, corresponding to ^{15}N in the $|\alpha\rangle$ and $|\beta\rangle$ spin states. The displacement in the $^{13}\text{C}'$ dimension then corresponds to $^1J(\text{C}'\text{--N})$, whereas that in the H^α dimension is $^3J(\text{H}^\alpha\text{--N})$. Provided the $^1J(\text{C}'\text{--N})$ splitting is resolved, the much smaller $^3J(\text{H}^\alpha\text{--N})$ is easily measured. Any change in ^{15}N spin state between the evolution of $^{13}\text{C}'$ magnetization and the end of $^1\text{H}^\alpha$ detection will result in a reduction of the apparent $^3J(\text{H}^\alpha\text{--N})$ splitting^{10,11} and it is therefore important that the passive nucleus (^{15}N) has a T_1 relaxation time which is long compared to the duration of the experiment. By conducting the HCACO experiment in D_2O , the backbone ^{15}N atoms are deuterated and have desirably long T_1 values of nearly 1 s. An alternative HN(CO)CA E.COSY type technique¹² requires that the spin state of H^α remains unchanged. However, as H^α changes its spin state relatively rapidly due to homonuclear NOE effects, use of a deuterated ^{15}N as a passive spin is preferred over that of $^1\text{H}^\alpha$. For measurement of $^3J(\text{H}^{\text{N}}\text{--C}')$, a HNCA E.COSY type experiment^{12,13} in which the carbonyl spin state remains unperturbed has been used. As the $^{13}\text{C}'$ spin relaxation is not dominated by a large one-bond $^{13}\text{C}\text{--}^1\text{H}$ interaction, its longitudinal relaxation time is relatively long (~ 1 s) and $^{13}\text{C}'$ T_1 relaxation therefore has minimal effect on the measured J coupling. To avoid confusion with a related HNCA E.COSY-based technique for measurement of $\text{H}^{\text{N}}\text{--H}^\alpha$ J couplings,¹⁴ we include the passive

[⊗] Abstract published in *Advance ACS Abstracts*, February 1, 1995.

(1) Karplus, M. *J. Chem. Phys.* **1959**, *30*, 11–15.

(2) Bystrov, V. F. *Prog. NMR. Spectrosc.* **1976**, *10*, 41–81.

(3) Pardi, A.; Billetter, M.; Wüthrich, K. *J. Mol. Biol.* **1984**, *180*, 741–751.

(4) Ludvigsen, S.; Andersen, K. V.; Poulsen, F. M. *J. Mol. Biol.* **1991**, *217*, 731–736.

(5) Vuister, G. W.; Bax, A. *J. Am. Chem. Soc.* **1993**, *115*, 7772–7777.

(6) Vijay-Kumar, S.; Bugg, C. E.; Cook, W. J. *J. Mol. Biol.* **1987**, *194*, 531–544.

(7) Griesinger, C.; Sørensen, O. W.; Ernst, R. R. *J. Chem. Phys.* **1986**, *85*, 6837–6843.

(8) Bax, A.; Vuister, G. W.; Grzesiek, S.; Delaglio, F.; Wang, A. C.; Tschudin, R.; Zhu, G. *Meth. Enzymol.* **1994**, *239*, 79–105.

(9) Grzesiek, S.; Bax, A. *J. Magn. Reson. Ser. B* **1993**, *102*, 103–106.

(10) Harbison, G. *J. Am. Chem. Soc.* **1993**, *115*, 3026–3027.

(11) Görlach, M.; Wittekind, M.; Farmer, B. T., II; Kay, L. E.; Mueller, L. *J. Magn. Reson. Ser. B* **1993**, *101*, 194–197.

(12) Seip, S.; Balbach, J.; Kessler, H. *J. Magn. Reson. Ser. B* **1994**, *104*, 172–179.

(13) Weisemann, R.; Rüterjans, H.; Schwalbe, H.; Schleucher, J.; Bermel, W.; Griesinger, C. *J. Biomol. NMR* **1994**, *4*, 231–240.

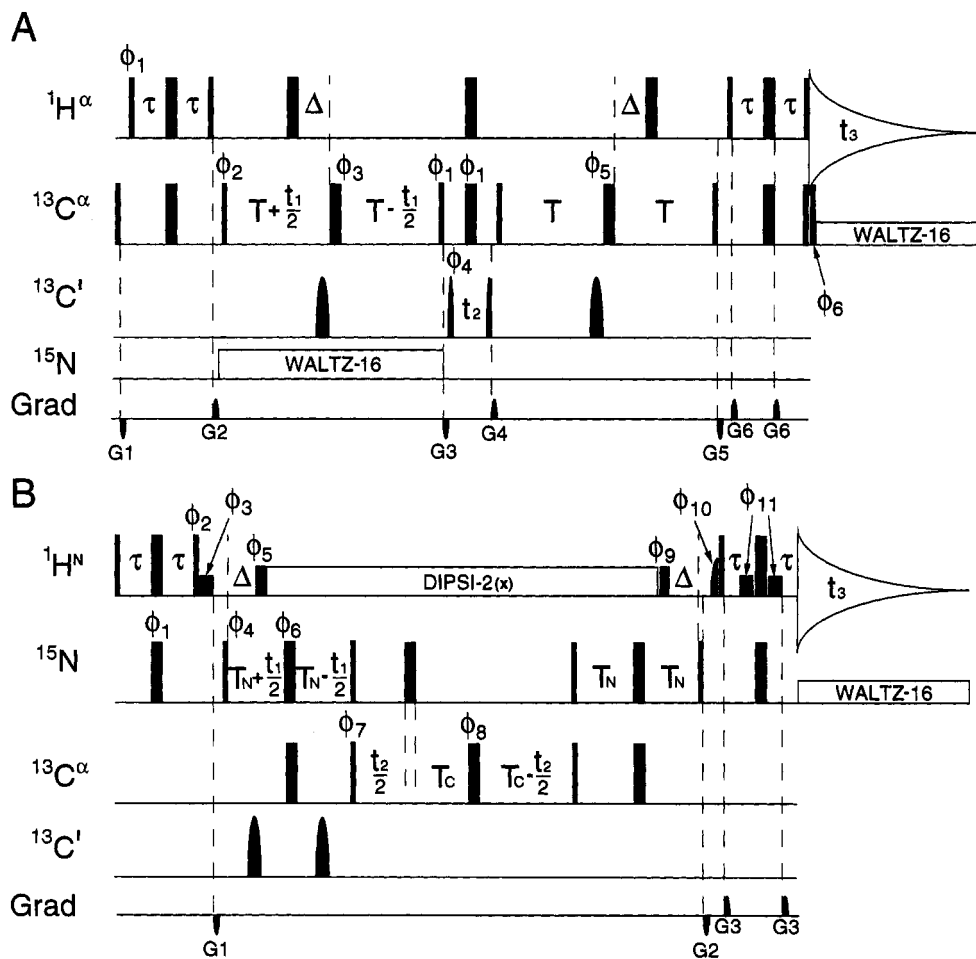


Figure 1. Pulse sequences of (A) the HCACO[N]-E.COSY and (B) the HNCA[CO]-E.COSY experiments. Pulses for which the phase is not indicated are applied along the x axis. The ^1H carrier is placed at the HDO frequency. The low power pulses in scheme B, with phases ϕ_3 , ϕ_5 , ϕ_9 , ϕ_{10} , and ϕ_{11} , all have 90° flip angles. For the remainder, narrow and wide pulses correspond to 90° and 180° flip angles, respectively. The carriers for the $^{13}\text{C}^\alpha$ and $^{13}\text{C}'$ pulses are positioned at 56 and 177 ppm, respectively. The RF field strengths of the 90° and 180° $^{13}\text{C}^\alpha$ pulses, 4.7 and 10.6 kHz, are adjusted such that they do not excite the $^{13}\text{C}'$ nuclei (for 150.9 MHz ^{13}C). Carbonyl pulses have a shaped amplitude profile, corresponding to the center lobe of a sinc/x function, and a duration of 157 and $84 \mu\text{s}$ for the 180° and 90° pulses, respectively. WALTZ-16 ^{13}C decoupling during data acquisition was performed using a 5 kHz RF field and ^{15}N WALTZ-16 decoupling with a 1.3 kHz RF field. For scheme A, phase cycling is as follows: $\phi_1 = y$; $\phi_2 = y$; $\phi_3 = 9^\circ, 9^\circ, 99^\circ, 99^\circ, 189^\circ, 189^\circ, 279^\circ, 279^\circ$; $\phi_4 = y, -y$; $\phi_5 = 9^\circ$; $\phi_6 = 4(x), 4(-x)$; Acq. = $x, -x, -x, x$. The application of a shaped $^{13}\text{C}'$ pulse prior to the $180^\circ_{\phi_3}$ $^{13}\text{C}^\alpha$ pulse causes a Bloch-Siegert shift on $^{13}\text{C}^\alpha$ during the application of this pulse, which leads to a phase shift which can be corrected for by increasing ϕ_3 by 9° . Depending on software and spectrometer type, a decrease in ϕ_3 may be required instead of an increase, or, alternatively, a second "Bloch-Siegert compensation" dummy pulse may be applied.¹⁹ Quadrature in the t_1 and t_2 domains is obtained by changing the phases ϕ_2 and ϕ_4 , respectively, in the usual States-TPPI manner. Delay durations are $\tau = 1.5$ ms, and $T = 3.3$ ms. Pulsed field gradients are sine-bell shaped, with a peak amplitude of 25 G/cm, and have durations of $G1 = 0.75$ ms, $G2 = 1.5$ ms, $G3 = 0.5$ ms, $G4 = 0.3$ ms, $G5 = 0.6$ ms, and $G6 = 0.2$ ms. $G1, G3,$ and $G5$ have negative polarity. For scheme B: $\phi_1 = x, -x$; $\phi_2 = y, -y$; $\phi_3 = x$; $\phi_4 = x$; $\phi_5 = y$; $\phi_6 = 4(x), 4(y), 4(-x), 4(-y)$; $\phi_7 = x, x, -x, -x$; $\phi_8 = 8(x), 8(y), 8(-x), 8(-y)$; $\phi_9 = -y$; $\phi_{10} = -x$; $\phi_{11} = -x$; Acq. = $P, -P, -P, P$, with $P = x, -x, -x, x$. Phases $\phi_3, \phi_9, \phi_{10}$, and ϕ_{11} are programmed on the AMX-600 as non-integral multiples of 90° in order to compensate for changes in phase associated with changes in power level. Quadrature in the t_1 and t_2 domains is obtained by changing the phases ϕ_4 and ϕ_7 , respectively, in the usual States-TPPI manner. Delay durations are $\tau = 2.25$ ms, $\Delta = 5.4$ ms, $T_N = 11$ ms, and $T_C = 14.29$ ms. Pulsed field gradient durations are $G1 = 1.5$ ms (negative polarity), $G2 = 1$ ms (negative polarity), and $G3 = 0.25$ ms. For scheme B, solvent suppression is accomplished by keeping the water magnetization along $+z$ between scans. This requires a combination of water flip-back pulses ($90_{\phi_3}, 90_{\phi_{10}}, 90_{\phi_{11}}$),²⁰ spin-locking the water magnetization along the x -axis ($90_{\phi_5}, \text{DIPSI-2}(x), 90_{\phi_9}$),²¹ and Watergate.²² Pulses with phases ϕ_3 and ϕ_{11} have a RF field strength of 143 Hz and the pulse with phase ϕ_{10} has a half-Gauss amplitude profile and a duration of 2.7 ms. Pulses with phases ϕ_5 and ϕ_9 and the DIPSI-2 ^1H decoupling are applied with a RF field strength of 5 kHz.

spin to which the J coupling is measured between square brackets in the name of the pulse sequence. The schemes used in the present study will therefore be referred to as HCACO[N]-E.COSY and HNCA[CO]-E.COSY.

Experimental Section

Two separate samples of uniformly $^{13}\text{C}/^{15}\text{N}$ enriched human ubiquitin (8.5 kDa) were used, 3.5 mg each in 220 μL Shigemi microcells

(14) Schmieder, P.; Thanabal, V.; McIntosh, L. P.; Dahlquist, F. W.; Wagner, G. J. *Am. Chem. Soc.* **1992**, *113*, 6323-6324.

(Shigemi Inc., Allison Park, PA) containing 30 mM sodium acetate buffer, pH 4.7. A D_2O sample was used for the HCACO[N]-E.COSY experiment and a H_2O sample for HNCA[CO]-E.COSY. All data were recorded at 30°C on a Bruker AMX-600 spectrometer, equipped with a triple resonance pulsed field gradient probehead. The HCACO[N]-E.COSY pulse sequence (Figure 1A) used in the present study differs from a previously described HCACO experiment⁹ by the omission of ^{15}N decoupling and pulsing and by additional pulsed field gradients. A $26^* \times 156^* \times 384^*$ 3D data matrix was acquired with acquisition times of 6.9 (t_1), 86.1 (t_2), and 127 ms (t_3). Data were zero filled to yield a digital resolution of 30 (F_1), 1.8 (F_2), and 0.74 Hz (F_3).

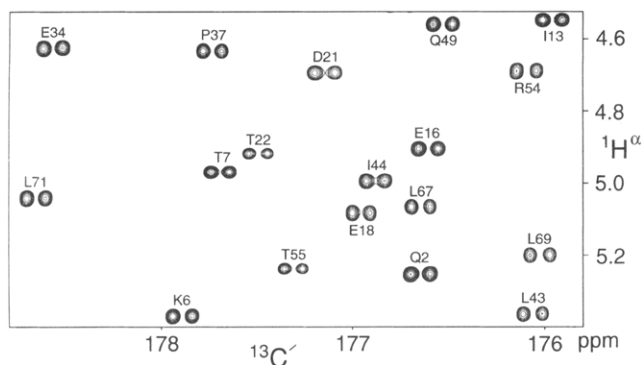


Figure 2. Small region of the 600 MHz 2D H(CA)CO[N]-E.COSY spectrum, recorded in the absence of ^{15}N decoupling. The spectrum shows intraresidue $\text{H}^\alpha\text{-C}'$ correlations in human ubiquitin. The horizontal splitting corresponds to $^1J(^{15}\text{N}\text{-}^{13}\text{C}')$, and the vertical displacement of the two doublet components is $^3J(^1\text{H}^\alpha\text{-}^{15}\text{N})$.

The HNCA[CO]-E.COSY pulse sequence (Figure 1B) is very similar to a scheme described by Weisemann et al.,¹³ except for the omission of shaped pulse C^α decoupling during H^N data acquisition (because of hardware malfunctioning at the time the data were recorded) and a slightly different approach to suppression of the H_2O resonance. The sequence yields distortion free spectra—a critical prerequisite for reliable J coupling measurement—but there is no indication that results of similar quality could not be obtained with the various sequences proposed by Weisemann et al.¹³ A $26^* \times 102^* \times 512^*$ 3D data matrix was acquired with acquisition times of 22 ms (t_1), 28 ms (t_2), and 65 ms (t_3). Data were zero filled to yield a digital resolution of 9.3 (F_1), 3.5 (F_2), and 1.9 Hz (F_3). Peak positions were determined using the program CAPP.¹⁵

Results and Discussion

The HCACO[N]-E.COSY experiment was carried out as both a 7-h 2D (without C^α chemical shift evolution) and a 45 h 3D experiment. A small region of the 2D HCACO[N]-E.COSY is shown in Figure 2. Fifty nine J couplings could be extracted from the 2D spectrum, and 67 values from the 3D. For the 59 J couplings for which two measurements are available, the pairwise rms difference is 0.16 Hz, indicating that the random error in their averaged value is 0.08 Hz. Measured $^3J(\text{H}^\alpha\text{-N})$ J values all fall in the -1.9 to 0.1 Hz range (supplementary material). Using singular value decomposition, coefficients A , B , and C are derived which give the best fit to the Karplus equation: $^3J(\text{H}^\alpha\text{-N}) = A \cos^2(\psi + 60^\circ) + B \cos(\psi + 60^\circ) + C$. The uncertainty in the coefficients is assessed by repeating the procedure 10 000 times, each time randomly omitting 10% of the measured data,⁵ resulting in $A = -0.88 \pm 0.03$, $B = -0.61 \pm 0.01$, $C = -0.27 \pm 0.03$. This Karplus curve, the measured data points, and the total range of Karplus curves obtained from the 10 000 fits are shown in Figure 3A. The present parametrization of the $^3J(\text{H}^\alpha\text{-N})$ Karplus curve is strikingly different from the original one, which was based on theoretical calculations and which predicted $^3J(\text{H}^\alpha\text{-N})$ values in the $+1.1$ to -6.6 Hz range. Kopple et al.¹⁶ and Barfield¹⁷ had pointed out previously that the original Karplus parametrization of this coupling provides poor results and the drastic change we find for A , B , and C therefore is not surprising. However, considering that the rms deviation of the measured data points (excluding couplings to Pro ^{15}N) from the Karplus

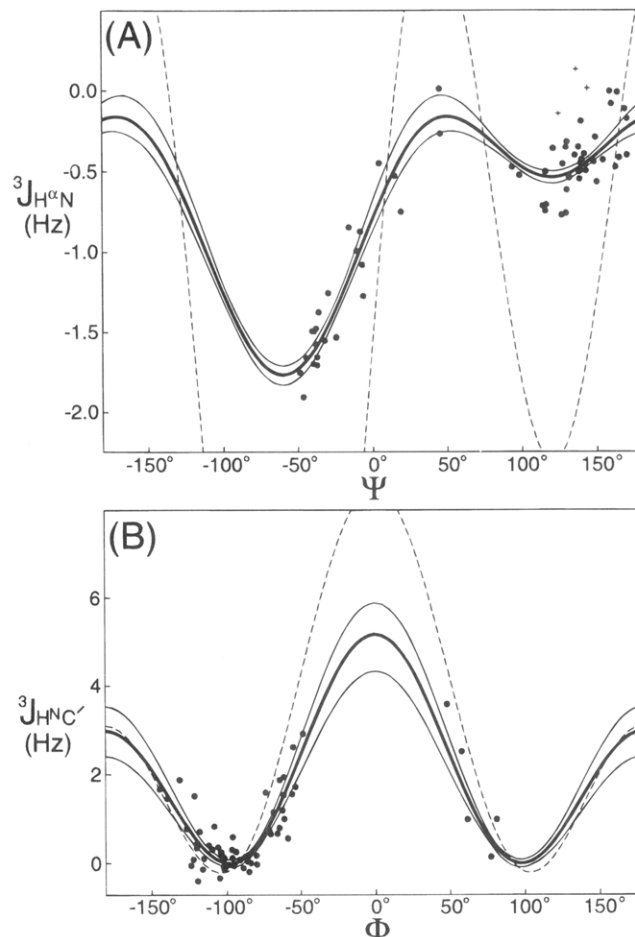


Figure 3. Karplus curves for (A) $^3J(^1\text{H}^\alpha\text{-}^{15}\text{N})$ and (B) $^3J(^1\text{H}^\text{N}\text{-}^{13}\text{C}')$. The heavy solid lines correspond to $^3J(\text{H}^\alpha\text{-N}) = -0.88 \cos^2(\psi + 60^\circ) - 0.61 \cos(\psi + 60^\circ) - 0.27$ and $^3J(\text{H}^\text{N}\text{-C}') = 4.0 \cos^2(\phi) + 1.1 \cos(\phi) + 0.1$. The thin solid lines mark the boundaries of a set of 10 000 Karplus curves, obtained by randomly deleting 10% fractions of the data points. The dashed lines correspond to previously commonly used parametrizations of these equations. Data points marked “+” are $^3J(^1\text{H}^\alpha\text{-}^{15}\text{N})$ couplings to proline ^{15}N , and have not been included in deriving the Karplus parametrization.

curve (0.16 Hz) is approximately 10 times smaller than the range of J couplings, $^3J(\text{H}^\alpha\text{-N})$ provides at least as good a measure for ψ as any other J coupling for other dihedral angles, despite its small magnitude. Unfortunately, in the $50^\circ < \psi < 180^\circ$ range $^3J(\text{H}^\alpha\text{-N})$ depends only weakly on ψ and therefore this coupling does not provide a good indicator for the value of ψ in regions of extended structure. In contrast to previous suggestions,¹⁸ it is possible to relate ψ to $^3J(\text{H}^\alpha\text{-N})$ without considering the other backbone angles ϕ and ω . Based on comparison of the $^3J(\text{H}^\alpha\text{-N})$ values measured in ubiquitin with those previously measured in small model compounds, it appears that $^3J(\text{H}^\alpha\text{-N})$ is sensitive to substituent effects. $^3J(\text{H}^\alpha\text{-N})$ values measured to the ^{15}N of the three prolines in ubiquitin appear to confirm this notion, as the $^3J(\text{H}^\alpha\text{-N})$ couplings to all three proline nitrogens (non-protonated) fall more than two standard deviations above the Karplus curve.

(18) DeMarco, A.; Llinas, M.; Wüthrich, K. *Biopolymers* **1978**, *17*, 647–650.

(19) Vuister, G. W.; Bax, A. *J. Magn. Reson.* **1992**, *98*, 428–435.

(20) Grzesiek, S.; Bax, A. *J. Am. Chem. Soc.* **1993**, *115*, 12593–12594.

(21) Kay, L. E.; Xu, G. Y.; Yamazaki, T. *J. Magn. Reson. Ser A* **1994**, *109*, 129–133.

(22) Piotto, M.; Saudek, V.; Sklenar, V. *J. Biomol. NMR* **1992**, *2*, 661–665.

(15) Garrett, D. S.; Powers, R.; Gronenborn, A. M.; Clore, G. M. *J. Magn. Reson.* **1991**, *94*, 214–220.

(16) Kopple, K. D.; Ashan, A.; Barfield, M. *Tetrahedron Lett.* **1978**, *38*, 3519–3522.

(17) Barfield, M. In *Recent developments in organic NMR Spectroscopy*; Lambert, J. B., Rittner, R., Eds.; Norell Press: Landisville, NJ, 1987; pp 65–74.

Sixty ${}^3J(\text{H}^{\text{N}}-\text{C}')$ couplings, obtained from the 3D HNCA[CO]-E.COSY measurement, fall in the -0.4 to 3.6 Hz range. The rms difference between the values measured from a 22 h 2D version of the experiment (without ${}^{15}\text{N}$ evolution) and the 3D experiment is 0.17 Hz, suggesting that the rms error in the 3D-derived ${}^3J(\text{H}^{\text{N}}-\text{C}')$ values is *ca.* 0.1 Hz. Optimal parametrization of the Karplus curve, ${}^3J(\text{H}^{\text{N}}-\text{C}') = A \cos^2(\phi) + B \cos(\phi) + C$, in the same manner as described above, yields $A = 4.01 \pm 0.14$, $B = 1.09 \pm 0.06$, and $C = 0.07 \pm 0.02$. The rms difference between measured J splittings and values predicted on the basis of this curve (Figure 3B) is 0.45 Hz. Although the original A , B , and C Karplus parameters (5.8 , -2.7 , 0.1) fall well outside the standard error of our new parametrization, use of the older curve (dashed line in Figure 3B) does not invalidate previous work based on qualitative interpretation of ${}^3J(\text{H}^{\text{N}}-\text{C}')$.

A protein of known structure provides an ideal "model compound" for parametrization of Karplus equations for all types of couplings that are of interest for protein structure determination by NMR. The deviation between measured J values and those predicted from the 1.8 \AA X-ray structure of

human ubiquitin does not show a significant increase in regions where the Karplus equation has its steepest angular dependence, suggesting that for ubiquitin the uncertainty in the crystallographically determined backbone angles is not limiting the accuracy at which the Karplus parameters can be determined.

Acknowledgment. We thank Frank Delaglio and Dan Garrett for developing the software used to process and analyze the NMR data. This work was supported by the AIDS Targeted Anti-Viral Program of the Office of the Director of the National Institutes of Health. A.C.W. is supported by an American Cancer Society postdoctoral fellowship (PF-4030).

Supplementary Material Available: One table containing the values of the ${}^3J(\text{H}^{\alpha}-\text{N})$ and ${}^3J(\text{H}^{\text{N}}-\text{C}')$ coupling constants (4 pages). This material is contained in many libraries on microfiche, immediately follows this article in the microfilm version of the journal, can be ordered from the ACS, and can be downloaded from the Internet; see any current masthead page for ordering information and Internet access instructions.

JA943275L